NeuroImage: Clinical 5 (2014) 120–127

Contents lists available at ScienceDirect

NeuroImage: Clinical

journal homepage: www.elsevier.com/locate/ynicl

Anatomical and diffusion MRI of deep gray matter in pediatric spina bifida

Ashley L. Ware[a,*], Jenifer Juranek[b], Victoria J. Williams[a], Paul T. Cirino[a], Maureen Dennis[c], Jack M. Fletcher[a]

[a]Department of Psychology, Texas Institute for Measurements, Evaluation and Statistics, University of Houston, 8201 Cullen St., Houston, TX 77204-6602, USA
[a]Department of Pediatrics, Children's Learning Institute BRAIN Lab, University of Texas Health Science Center at Houston, 6655 Travis Street Suite 1000, Houston, TX 77030, USA
[a]Program in Neurosciences and Mental Health, The Hospital for Sick Children, 555 University Avenue, Toronto, Ontario, Canada

ARTICLE INFO

Article history:
Received 19 February 2014
Received in revised form 15 May 2014
Accepted 20 May 2014
Available online 2 June 2014

Keywords:
Myelomeningocele
Hydrocephalus
Subcortical gray matter
DTI

ABSTRACT

Individuals with spina bifida myelomeningocele (SBM) exhibit brain abnormalities in cortical thickness, white matter integrity, and cerebellar structure. Little is known about deep gray matter macro- and microstructure in this population. The current study utilized volumetric and diffusion-weighted MRI techniques to examine gray matter volume and microstructure in several subcortical structures: basal ganglia nuclei, thalamus, hippocampus, and amygdala. Sixty-six children and adolescents (ages 8–18; M = 12.0, SD = 2.73) with SBM and typically developing (TD) controls underwent T_1- and diffusion-weighted neuroimaging. Microstructural results indicated that hippocampal volume was disproportionately reduced, whereas the putamen volume was enlarged in the group with SBM. Microstructural analyses indicated increased mean diffusivity (MD) and fractional anisotropy (FA) in the gray matter of most examined structures (i.e., thalamus, caudate, hippocampus), with the putamen exhibiting a unique pattern of decreased MD and increased FA. These results provide further support that SBM differentially disrupts brain regions whereby some structures are volumetrically normal whereas others are reduced or enlarged. In the hippocampus, volumetric reduction coupled with increased MD may imply reduced cellular density and aberrant organization. Alternatively, the enlarged volume and significantly reduced MD in the putamen suggest increased density.

1. Introduction

Spina bifida myelomeningocele (SBM), identified by the herniated protrusion of the spinal cord and meninges from the vertebrae at birth (Detrait et al., 2005), is the most common congenital birth defect affecting the central nervous system compatible with survival. It occurs in approximately .3–.5 per 1000 live births (Au et al., 2010). Almost all individuals with SBM incur structural brain abnormalities, including variable anomalies of the midbrain and corpus callosum. Most consistently observed is the Chiari II malformation of the hindbrain, which occurs in over 90% of cases with SBM (Juranek and Salman, 2010). Resultant obstruction at the level of the fourth ventricle leads to hydrocephalus in the majority (roughly 80%) of people with SBM, with many receiving shunt diversion as treatment.

The high comorbidity of hydrocephalus and shunt treatment in individuals with SBM disrupts brain macro- and microstructure (Del Bigio, 2010), leading to variable neural and cognitive outcomes (Hampton et al., 2011). Although intellectual disability is infrequent in SBM, the neurobehavioral profile of SBM consists of strengths in lower-order cognitive and motor domains, such as association and motor learning. Weaknesses are in higher-order, contextually based cognitive processes, including problem solving and on-line information integration (Dennis and Barnes, 2010). There are often relative strengths in motor learning and adaptation to environmental stimuli, but weaknesses in dynamic motor regulation such as impaired movement coordination and fine motor control (reviewed in: Dennis and Barnes, 2010).

Given the characteristic features of the Chiari II malformation and motor impairments, initial neuroimaging studies of SBM targeted cerebellar abnormalities, revealing generally reduced cerebellar volumes in these individuals relative to typically developing (TD) peers (Dennis et al., 2004; Juranek and Salman, 2010). However, despite overall volume reductions, individuals with SBM show significant volumetric enlargement in anterior cerebellar portions and reductions in posterior–inferior regions (Juranek et al., 2008).

At the level of the cerebrum, individuals with SBM also exhibit anterior to posterior patterning in the cortex as well as in the corpus callosum (Hannay et al., 2009; Hannay et al., 2008; Juranek et al., 2008; Treble et al., 2013). Cortical thickness is significantly increased in frontal regions, but decreased in posterior regions (Juranek et al.,

* Corresponding author.
E-mail addresses: aware2004@gmail.com (A.L. Ware), Jenifer.Juranek@uth.tmc.edu (J. Juranek), tori85@gmail.com (V.J. Williams), Paul.Cirino@times.uh.edu (P.T. Cirino), Maureen.dennis@sickkids.ca (M. Dennis), Jack.Fletcher@times.uh.edu (J.M. Fletcher).

http://dx.doi.org/10.1016/j.nicl.2014.05.012

2008). When examining cortical complexity (i.e., gyrification) a similar pattern emerges whereby frontal regions generally have significantly less complexity (except the middle frontal region) despite significantly greater complexity in parietal and temporal cortices relative to TD controls (Treble et al., 2013). Posterior regions of the corpus callosum may also be more affected in SBM; the genu is generally well preserved whereas the splenium shows the greatest dysgenesis (Hannay et al., 2009).

White matter (WM) and gray matter (GM) volumetric and microstructural alterations also exist in individuals with SBM. WM integrity is particularly reduced in long association fiber tracts connecting posterior and anterior brain regions (Hasan et al., 2008a; Ou et al., 2011). Most studies have reported decreased fractional anisotropy (FA) and increased mean diffusivity (MD) in SBM relative to controls (Ou et al., 2011; Hasan et al., 2008a; Williams et al., 2013). Lower FA has also been observed in the genu of the corpus callosum, but not in the anterior commissure (Herweh et al., 2009). In a recent probabilistic tractography study of attention pathways in SBM, posterior pathways showed greater reduction in WM integrity (decreased FA) than frontal pathways (Williams et al., 2013). Tectal beaking occurs with high frequency in people with SBM and was further associated with WM alterations in both anterior and posterior attention pathways. Limbic tract integrity, as previously examined through fiber tracking and region of interest (ROI) techniques, is also reduced in SBM, particularly in the fornix and cingulum (Kumar et al., 2010; Ou et al., 2011; Vachha et al., 2006).

Little is known about deep GM structure and integrity in SBM. This knowledge is relevant given disruptions in periventricular white matter, the fornix, and long association fibers, which have connections with subcortical GM structures such as basal ganglia nuclei and the hippocampus. However, no studies to our knowledge have examined specific limbic system structures and few have investigated the thalamus and basal ganglia structures. Of the three studies that have investigated specific basal ganglia nuclei and periventricular GM regions using quantitative methods, the most consistent finding is reduced GM integrity in the caudate nucleus of the basal ganglia (Hasan et al., 2008b; Kumar et al., 2010; Kumar et al., 2011). However, discrepancies exist between these three studies of GM integrity. While decreased FA and increased MD values were observed in the caudate nucleus of children with SBM relative to controls in one study (Kumar et al., 2010), two other studies reported increased FA in this region relative controls (Hasan et al., 2008b; Kumar et al., 2011).

Similarly, some discrepancies exist with regard to published reports of putamen integrity. One study reported no significant differences in SBM compared to controls in DTI metrics of the putamen (Hasan et al., 2008b) and another study reported increased FA in this structure (Kumar et al., 2011). Kumar et al. (2011) also investigated GM integrity of the thalamus, but reported no significant differences between patients and controls (Kumar et al., 2011), despite its proximal location to periventricular WM, which has abnormal features in SBM (Hasan et al., 2008a). To date, no studies have examined whether volumetric differences in these regions (i.e., limbic, basal ganglia, thalamus) are evident in SBM. The clinical implications of elucidating subcortical GM volume and integrity differences are relevant since most GM structures are clinically read as "normal" during qualitative radiological review (Fletcher et al., 2005).

To further understand subcortical GM in SBM and clarify current discrepancies in existing literature, we examined the volumetric and microstructural properties of deep GM regions in SBM and a typically developing comparison group.

1.1. Hypotheses

1 Volumetric measures (corrected for total brain volume) of deep GM structures will be systematically *reduced* in participants with SBM relative to TD controls.

2 Measures of microstructure in deep GM will reflect reduced (indicated by increased mean diffusivity and reduced fractional anisotropy) integrity of these regions in participants with SBM relative to typically developing controls.

2. Materials and methods

2.1. Participants

Participants included children and adolescents ($N = 66$) between 8 and 18 years ($M = 12.0$, $SD = 2.73$) of age with SBM ($n = 48$) and typically developing controls (TD; $n = 18$). Participants were drawn from the Houston cohort of an international project examining neurobehavioral outcomes of spina bifida (Fletcher et al., 2005). While participants with SBM were recruited from clinics at Texas Children's Hospital and Shriners Hospital for Children, TD participants were recruited from advertisements and community contacts and had no previous or current neurological difficulties. Participants with SBM had hydrocephalus (20.8% mild at time of testing) and all but one had been treated with a shunt near the time of birth. Most participants with SBM had lumbar and sacral spinal lesions (83.3%), Chiari II malformation (87.5%), callosal hypogenesis or hypoplasia (thinning) (95.8%), less than 5 shunt revisions (81.2%), and infrequent seizure history (none: 66.7%; past: 8.3%; current: 4.2%).

Participants in both groups had verbal and/or nonverbal intelligence quotient (IQ) scores between 70 and 120 per the Stanford–Binet Intelligence Scale: Fourth Edition (Thorndike et al., 1986). Full-scale IQ estimates ranged between 63 and 112 for the group with SBM and between 84 and 120 for the TD group. Some children with lower IQ scores were eliminated from the parent study because of concerns about their capacity for following directions on neuropsychological assessment procedures and are not discussed below. All study procedures, including MRI acquisitions, were conducted between 2005 and 2010 and were in compliance with IRB approval at The University of Houston and The University of Texas Health Science Center at Houston.

Demographic characteristics of the sample are displayed for each group in Table 1. As expected, participants with SBM had significantly lower verbal and nonverbal IQ scores ($ps \leq .001$) than controls and significantly lower socioeconomic status (SES) per the Four Factor Index of Social Status (Hollingshead, 1975). The group with SBM also had a greater number of non-right handed individuals, which is common in samples of SBM (Fletcher et al., 2005) and other samples involving congenital brain injury (e.g., Ross et al., 1987).

2.2. Magnetic resonance image acquisition

All MRI acquisitions were acquired at the University of Texas Medical School in Houston using a research-dedicated Philips 3 T scanner with SENSE (Sensitivity Encoding) technology and an 8-channel phased array head coil.

2.2.1. T_1-weighted imaging

After a conventional scout sequence, high-resolution T_1-weighted anatomical images were acquired in the coronal plane using a 3D turbo fast echo sequence with the following parameters: voxel dimensions = .94 × .94, slice thickness = 1.5 mm, TR = 6.50–6.70 ms, TE = 3.04–3.14 ms, flip angle = 8°, DFOV = 240 mm, matrix = 256 × 256.

2.2.2. Diffusion tensor imaging (DTI)

DTI images were acquired in the axial plane using a single-shot spin-echo diffusion sensitized echo-planar imaging sequence. Diffusion sensitizing gradients were applied in 21 directions (weighting: $b = 1000$ s/mm^2) with one reference image ($b = 0$ s/mm^2) and the following parameters: voxel dimensions = .94 × .94 mm, slice thickness = 3 mm,

Table 1
Demographic data for the spina bifida myelomeningocele (SBM) and typically developing control (TD) groups.

Variable	SBM ($n = 42$)	TD ($n = 18$)	p-Value	Pairwise
Sex (n [% male])	24 (57.1)	11 (61.1)	.421	
Handedness (n [% right])	35 (72.9)	16 (88.9)	.051	TD > SBM
Age at MRI (M [SD])	12.34 (2.9)	11.24 (2.2)	.148	
Ethnicity (n [% Hispanic])	28 (58.3)	14 (77.8)	.282	
Socioeconomic status (M [SD])*	31.36 (13.2)	39.83 (11.3)	.018	TD > SBM
Full-scale IQ (M [SD])	85.23 (12.4)	104.18 (10.3)	<.001	TD > SBM
Verbal IQ (M [SD])	85.54 (16.0)	99.56 (13.0)	.001	TD > SBM
Nonverbal IQ (M [SD])	92.00 (14.1)	107.44 (14.1)	<.001	TD > SBM

Note: IQ and socioeconomic status estimates obtained from the Stanford–Binet Intelligence Scales and Four Factor Index of Social Status, respectively (Thorndike et al., 1986; Hollingshead, 1975).

TR = 6500 ms, TE = 65 ms, flip angle = 90°, DFOV = 240 mm, matrix = 256 × 256.

2.3. Magnetic resonance data analysis

All scans underwent initial radiological evaluation. The basal ganglia structures (i.e., caudate, putamen, globus pallidus) were all read as "normal" for both groups and the thalamus was read as normal for all participants in the TD group and for 95.8% of participants in the group with SBM (2 showed unilateral abnormality and 1 had massa intermedia < 1 cm).

Prior to data preprocessing, anatomical MRI and DTI data were reviewed for image quality by an expert user with extensive neuroimaging knowledge and experience (JJ) who was blind to age, gender, and neuropsychological performance outcomes. Morphometric analyses were conducted in FreeSurfer v4.0.5 (*http://www.surfer.nmr.mgh.harvard.edu*) (Fischl, 2012) using a 64-bit Linux computer. Skull-stripping and regional segmentation were executed using a fully automated command (e.g., recon-all –all) for each T_1-weighted image, yielding 3 classes of voxels: gray matter (GM), white matter (WM), and cerebrospinal fluid (CSF) (Fischl et al., 2002; Fischl et al., 2004a; Fischl et al., 2004b). Subsequently, within FreeSurfer, a fully automated routine determined delimiting boundaries of deep GM structures (i.e., caudate, putamen, pallidum, thalamus, hippocampus, amygdala). The brains of people with SBM are dysmorphic and boundaries are not always reliably indicated by the FreeSurfer output. The output images from FreeSurfer's segmentation and classification algorithms were visually inspected and extensively manually edited by a single rater (JJ) with substantial expertise using FreeSurfer's software as well its predecessor, Cardviews (Filipek et al., 1989). An example of finalized segmentation after manual editing is shown in Fig. 1. At the time of MRI acquisitions (collected between 2005 and 2010), FreeSurfer v4.0.5 (released June 2008) was the most recent version available for analyses. Although subsequent revisions of FreeSurfer were released, FreeSurfer v5.0.0 (released in 2010) was the first version that retained manual edits (i.e., persistent edits) and the older version of FreeSurfer was maintained to ensure consistency across study subjects.

For DTI data, within-participant co-registration of the GM masks (obtained from the FreeSurfer analyses) in T_1-space with DTI space (B0 or nodif image) were performed using FSL v4.1.0 (FMRIB's Software Library, *http://www.fmrib/ox.ac.uk/fsl*) (Smith et al., 2004). Minor head motion and eddy currents were corrected in the DTI series with the Eddy Current Correction tool included in FSL's Diffusion Toolbox v2.0. Skull-stripping and removal of non-brain tissue were performed using BET v2.1. FSL's Linear Image Registration Tool v5.5 (FLIRT) (Jenkinson et al., 2002) was used to perform a within-participant inter-modal linear registration between each participant's T_1-weighted series (reference image) and corresponding non-diffusion-weighted images ($b = 0$) from the DTI dataset. The resultant transformation matrix (and calculated inverse) was used to transform the binary segmentation masks of each GM structure (obtained from high-resolution T_1-weighted images using FreeSurfer) to corresponding diffusion-weighted space (detailed in Juranek et al., 2012). The diffusion tensors were reconstructed using FSL's DTIFIT tool within the Diffusion Toolbox. This transformation matrix was then applied to each participant to mask individual maps of MD and FA for each GM structure. To be as conservative as possible, each participant's binary segmentation mask was eroded using a $2 \times 2 \times 2$ mm^3 kernel to reduce contamination from neighboring voxels of CSF and/or WM. Final quantitative data were obtained using command line utilities to compute average MD and FA circumscribed by each eroded deep GM mask in each participant.

2.4. Data analyses

Preliminary analyses included examination of the distributions of the primary volumetric and DTI variables within and across groups and evaluation of hemispheric differences by group in addition to potential covariates and moderators (e.g., age, sex). IQ was not considered as an appropriate covariate. A covariate that is an attribute or an intrinsic characteristic of the condition cannot be meaningfully adjusted to

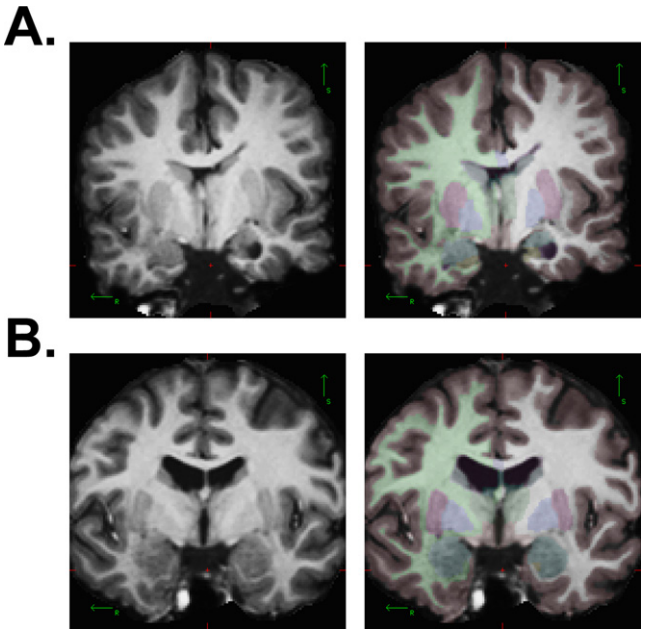

Fig. 1. Examples of final segmentations following extensive manual edits. A) SBM participant's T1-weighted MRI (left panel) with color-coded segmentation boundaries of deep gray matter structures (right panel). B) TD participant's T1-weighted MRI (left panel) with color-coded segmentation boundaries of deep gray matter structures (right panel).

"control" for the attribute, instead creating groups with artificial mean differences reflecting the association of the covariate with the disorder (Dennis et al., 2009). In addition, handedness was not included as a covariate given the lack of variance in the TD group (Kutner et al., 2005).

Across groups, distributions of volumetric data were generally normal. Within groups, large deviations from group means (˜2 SD) were rare, but where they occurred, they were specifically evaluated for impact. The group with SBM had significantly smaller total brain volume (TBV) relative to the TD group, $F(1,64) = 24.40$, $p < .001$. Therefore volumetric measures were evaluated using corrected ratios (GM structure volume to TBV) for all analyses.

To examine potential hemispheric differences between groups, separate 2 (hemisphere: left, right) × 2 (group: SBM, TD) repeated measures ANOVAs were examined for each corrected GM volume and DTI value (MD, FA). With the exception of thalamus volumes ($p = .031$), none of the group × hemisphere interactions were significant for GM volumes or DTI metrics ($p > .05$). Across groups, there were significant hemisphere effects ($p < .015$) found for volumes of pallidum and putamen, FA in all basal ganglia structures (caudate, pallidum, putamen), and MD in the amygdala, pallidum, and putamen. However, since none of the group × hemisphere interaction effects were significant, indicating similar lateralization of volumetric and DTI metric values for participants in the SBM and TD groups, hemisphere was not included in the main analyses below. There were also no significant group × hemisphere × sex interactions, indicating hemispheric similarity for males and females. Given these findings, whole corrected GM structure volumes (average of left and right hemispheres) and DTI values were computed for each GM structure and examined in subsequent analyses, with the exception of thalamus volumes.

Across groups, age was not significantly correlated ($r < .190$) with GM volumes, although when groups were examined separately age was associated with putamen volumes in the TD, but not in the group with SBM. However, age was significantly associated with microstructure values both across and within groups separately. Since the literature has shown age effects on GM volume and microstructure values across development (e.g., Lebel et al., 2008), it was included as a covariate in all analyses.

To address the study hypotheses, two sets of results were examined, first comparing deep GM volumes and then DTI values between the SBM and TD groups on each structure. Each deep GM structure was examined using separate ANCOVAs with group (SBM, TD) entered as the independent variable. For thalamus volume, for which there was a significant group × hemisphere interaction, a 2-way repeated measure ANCOVA with one repeated factor (hemisphere) and one between-subjects factor (group) was utilized. For all models, age was included.

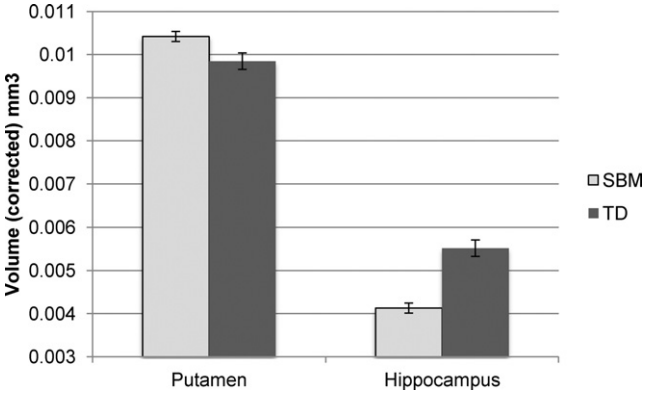

Fig. 2. Group differences on corrected putamen ($p = .005$) and hippocampus ($p < .001$) volumes between participants with spina bifida myelomeningocele (SBM; $n = 48$) and typically developing controls (TD; $n = 18$). Values reflect averages between left and right hemispheres. Note: bars represent standard error.

3. Results

3.1. Macrostructure

Table 2 presents means and standard deviations for each deep GM structure volume (with and without correction for TBV, which differed between groups). ANCOVA results (with covariate age) indicated significant effects (shown in Fig. 2) of group for volumes of the putamen, $F(1,63) = 8.55$, $p = .005$, $\eta^2_{partial} = .119$, and hippocampus, $F(1,63) = 39.73$, $p < .001$, $\eta^2_{partial} = .387$, but not for the pallidum, amygdala, or caudate, $F(1,63) < 1$, $p \geq .335$. Participants with SBM had smaller hippocampi and larger putamen volumes. Age was only significantly positively associated with putamen volume, $F(1,63) = 5.05$, $p = .028$, $\eta^2_{partial} = .074$.

For the thalamus, the effects of hemisphere and hemisphere × age were not significant (*ps* ≥ .593), although the hemisphere × group effect was significant, $F(1,63) = 4.25$, $p = .043$, $\eta^2_{partial} = .063$. For the between-group effects, neither age nor group was statistically significant (*ps* ≥ .274). Follow-up examination of the hemisphere × group interaction revealed a greater, though nonsignificant (*ps* ≥ .139), discrepancy between groups (SBM > TD) in the left (M[SD]: SBM = .0063 [.0011]; TD = .0059 [.0005]) relative to the right (M [SD]; SBM = .0061 [.0009]; TD = .0060 [.0005]) thalamus.

Table 2
Mean (standard deviations) for raw and corrected (raw to total brain volume) deep gray matter structures for participants with spina bifida myelomeningocele (SBM; $n = 48$) and typically developing controls (TD; $n = 18$). Values reflect averages between left and right hemispheres.

	Raw volume (mm^3)		Corrected volume (mm^3)		
Brain region	SBM	TD	SBM	TD	Pairwise (corrected)
Total brain volume	1,183,298.86 (97,723.81)	1,291,996.14 (83,270.50)			SBM < TD ***
Hippocampus	4845.14 (1060.48)	7034.00 (812.60)	.004 (.0009)	.005 (.0007)	SBM < TD ***
Amygdala	3699.86 (684.60)	3961.27 (419.55)	.003 (.0006)	.003 (.0003)	
Caudate	7434.11 (1147.82)	7912.05 (812.64)	.006 (.0008)	.006 (.0006)	
Putamen	12,302.23 (1442.31)	12,731.45 (1007.44)	.0104 (.0010)	.010 (.0006)	SBM > TD **
Pallidum	3682.62 (594.91)	3944.68 (586.11)	.003 (.0005)	.003 (.0004)	SBM > TB *+
Thalamus++	14,910.35 (2430.92)	15,743.18 (1856.24)	.013 (.0021)	.012 (.0012)	

Note: reported values reflect the average volume for left and right hemispheres.
+ Group differences for pallidum volume were no longer significant after demographic variables (sex, socioeconomic status) were included as covariates.
++ Between-group differences on thalamus volumes were examined using a 2 (group) × 2 (hemisphere) within-participants ANCOVA.
* $p \leq .05$.
** $p \leq .01$.
*** $p \leq .001$.

Table 3
Means (standard deviations) of DTI values for the spina bifida myelomeningocele (SBM, $n = 49$) and typically developing control (TD, $n = 18$) groups.

	Mean diffusivity			Fractional anisotropy		
Brain region	SBM	TD	Pairwise	SBM	TD	Pairwise
Hippocampus	1.089 (.127)	0.954 (.056)	SBM > TD ***	0.178 (.044)	0.168 (.048)	
Amygdala	0.894 (.014)	0.855 (.139)		0.209 (.030)	0.186 (.016)	SBM > TD **
Caudate	0.789 (.049)	0.751 (.015)	SBM > TD ***	0.163 (.030)	0.125 (.016)	SBM > TD ***
Putamen	0.745 (.015)	0.756 (.011)	SBM < TD *	0.158 (.017)	0.143 (.012)	SBM > TD ***
Pallidum	0.765 (.029)	0.774 (.019)		0.301 (.033)	0.244 (.027)	SBM > TD ***
Thalamus	0.799 (.035)	0.775 (.022)	SBM > TD **	0.302 (.020)	0.275 (.014)	SBM > TD ***

Note: MD M (SD) reported with values $\times 10^{-3}$; reported values reflect the average MD/FA for left and right hemispheres.
* $p < .05$.
** $p \leq .01$.
*** $p \leq .001$.

3.2. Microstructure

Results for microstructure (MD and FA) are presented in Table 3. Only overall models and effects that met critical level of alpha ($p < .05$) are discussed below.

3.2.1. Mean diffusivity

There was a significant effect of group on MD values in the thalamus, $F(1,63) = 9.26$, $p = .003$, $\eta^2_{partial} = .128$, caudate, $F(1,63) = 12.57$, $p = .001$, $\eta^2_{partial} = .166$, putamen, $F(1,63) = 5.12$, $p = .027$, $\eta^2_{partial} = .075$, and hippocampus, $F(1,63) = 19.67$, $p < .001$, $\eta^2_{partial} = .238$. MD was significantly higher for the group with SBM in the thalamus, caudate and hippocampus and significantly lower in the putamen relative to the TD group. Age was significantly negatively associated with MD in the putamen, $F(1,63) = 6.08$, $p = .016$, $\eta^2_{partial} = .088$, and pallidum, $F(1,63) = 21.19$, $p < .001$, $\eta^2_{partial} = .252$.

3.2.2. Fractional anisotropy

There was a significant effect of group on FA values in the thalamus, $F(1,63) = 24.34$, $p < .001$, $\eta^2_{partial} = .279$, putamen, $F(1,63) = 11.22$, $p = .001$, $\eta^2_{partial} = .151$, caudate, $F(1,63) = 25.34$, $p < .001$, $\eta^2_{partial} = .287$, pallidum, $F(1,63) = 39.46$, $p < .001$, $\eta^2_{partial} = .385$, and amygdala, $F(1,63) = 10.92$, $p = .002$, $\eta^2_{partial} = .148$. FA was significantly higher for the group with SBM in all structures relative to the TD group. Age was significantly positively associated with FA in the pallidum, $F(1,63) = 4.57$, $p = .036$, $\eta^2_{partial} = .068$, and in the thalamus, $F(1,63) = 15.25$, $p < .001$, $\eta^2_{partial} = .195$.

3.3. Sex and socioeconomic status as covariates

3.3.1. Sex

Given the potential sex differences in GM volumes and microstructural metric values, sex was added to the original model as a covariate along with age. With covariates sex and age, volumetric results remained similar except for reduced group differences in pallidum volumes ($p = .551$); groups remained significantly different on hippocampus ($p < .001$) and putamen ($p = .004$) volumes. Group differences on MD values did not meet the critical value of alpha for the pallidum and amygdala, but remained significant in the putamen ($p = .047$), caudate ($p = .001$), thalamus ($p = .004$), and hippocampus ($p < .001$). The addition of sex as a model covariate also did not change results for FA values in any region; all deep GM structures, except the thalamus, had increased FA in the group with SBM relative to the TD group ($p \leq .001$).

3.3.2. Socioeconomic status

Results were also not substantially altered by the addition of SES as a model covariate. When both age and SES were controlled, group differences in GM region volume remained similar, with the exception of pallidum volume ($p = .717$). The hippocampus remained significantly reduced and the putamen remained significantly enlarged in the group with SBM compared to controls. The additional covariate also did not substantially alter any of the findings for MD or FA; significant group differences in MD persisted in all regions except the amygdala and pallidum and groups remained significantly different on FA values in all structures except the hippocampus.

3.4. Examination of shunt status in the group with SBM.

Given that all but one participant in the group with SBM had received shunt intervention as treatment for hydrocephalus, the number of shunt revisions was examined as a predictor for GM volumes and MD and FA. Linear regression was used to predict whether more revisions resulted in smaller corrected volumes and worse integrity compared to fewer shunt revisions for all examined GM regions. For participants with SBM, regression results indicated that number of shunt revisions was not strongly associated with GM volumes ($p \geq .264$), FA values ($p \geq .148$), or MD values ($p \geq .080$).

4. Discussion

Failure of neural tube closure in utero results in an altered pattern of programmed fetal development leading to gross anatomical brain dysmorphologies. In SBM, the considerable inter-individual variability in measures of both structure and function is documented (Fletcher et al., 2005). The present study probed distinct structural properties (both macro- and microstructural indices) of deep GM in children and adolescents with SBM relative to a TD comparison group.

Contrary to initial expectations of ubiquitous disproportionate reduction in volume and microstructural integrity of subcortical GM structures following SBM, findings (summarized in Tables 2 and 3) supported a model of regionally specific GM areas being differentially impacted by this early gestational insult. Whereas the hippocampus showed volumetric reduction, the putamen was significantly enlarged. The majority of other GM structures (i.e., thalamus, amygdala, caudate, globus pallidus) were volumetrically scaled to TBV in both groups. Similarly, results from the DTI metrics (i.e., MD, FA) suggested that deep GM microstructural integrity was not uniformly disrupted in SBM. Significant group differences across structures typically followed a pattern where the group with SBM showed increased MD values. Three exceptions were in the putamen, where MD was decreased, and in the amygdala and pallidum, which had similar values between groups. With respect to FA values, all evaluated structures (except the hippocampus) demonstrated significant group differences with increased FA values in the group with SBM relative to controls.

These findings are consistent with the overall concept that SBM results in a complex pattern of disproportionate *enlargement* in some regions (e.g., volume of the putamen and anterior cerebellum and prefrontal cortical thickness and complexity), disproportionate *reduction* of volume in other regions (e.g., the hippocampus and inferior–posterior cerebellum and parietal cortical thickness), in conjunction with typical structure of some brain regions (Juranek and Salman, 2010).

The anomalous structural patterning in SBM may reflect complex compensatory mechanisms of neural plasticity in this population. Additionally, the mechanical effects of hydrocephalus likely complicate the protracted brain development in SBM.

The hippocampus may be particularly affected in SBM given the disproportionately reduced volume and increased MD observed relative to controls. Volumetric reduction coupled with increased MD could imply lower cellular density and/or aberrant cellular structure and organization in SBM. The hippocampus develops early in gestation (with individual subfields distinguishable around 15–19 weeks) and is particularly sensitive to early gestational factors associated with the occurrence of SBM, including malnutrition (Arnold and Trojanowski, 1996; Morgane et al., 2002) and mechanical injury due to hydrocephalus (Del Bigio, 2010). Previous studies in clinical and preclinical populations indicate thinning and stretching of the fimbria and fornix (Del Bigio et al., 2003; Naidich et al., 1982), which likely disrupts subcortical and collosal connectivity of the hippocampus (Del Bigio and Zhang, 1998; Mataro et al., 2006). Microstructural abnormalities of cellular deterioration in axons and synapses in hydrocephalic animal models further support the current interpretation of diminished cell density and structural organization of the hippocampus in the group with SBM (Kriebel and McAllister, 2000). Thus, the macro- and microstructural integrity of the hippocampus in SBM may reflect initial damage resulting from failure of neural tube closure coupled with prolonged damage resulting from hydrocephalus.

The putamen reflected a unique profile of increased volume, increased FA, and decreased MD in the group with SBM. The disproportionately increased volume and significantly reduced MD values observed in the putamen are not indicative of decreased density, but rather increased density. The literature of typical development from childhood to late adolescence and adulthood supports negative relations between age and MD values in the putamen (e.g., Abe et al., 2008; Lebel et al., 2008; Mukherjee et al., 2002). However, typical development of subcortical gray matter volumes generally peaks in early adolescence and decreases into young adulthood (Giedd et al., 1999a; Giedd et al., 1999b; Good et al., 2001; Ostby et al., 2009). When taken together with the larger volumes observed in the putamen, potential explanations for group differences in MD include atypical structural organization and aberrant apoptosis, or programmed cell death that typically occurs across adolescence. Mukerjee et al. (2002) suggested that deviations from isotropy could reflect deviations in structural patterning during neuronal and glial arborization, which supports our interpretation of increased FA and decreased MD in the current sample with SBM (Mukherjee et al., 2002). However, lack of research in early brain structure of infants and young children with SBM complicates elucidation of group differences. Knowledge of early brain macro- and microstructure in SBM would increase current understanding regarding structural and maturational anomalies in SBM.

Surprisingly, the current analyses also indicated distinct volumetric and microstructural patterning between the putamen and caudate in SBM. Structural properties of the caudate and the putamen (or dorsal striatum) were expected to be similar given the common embryonic derivation of these structures from the transient ventricular eminence (e.g., telencephalic origin) early in gestation (Marín and Rubenstein, 2003). In contrast, the globus pallidum emerges from diencephalic origins (Müller and O'Rahilly, 2006) and migrates to its final telencephalic position in the median eminence which together with the lateral eminence forms the floor of the third ventricle (Müller and O'Rahilly, 2006). Thus, structural properties of the caudate and the putamen are expected to be very similar since neurons within their boundaries are derived from the same origin. In contrast, structural properties of the pallidum are not expected to share structural similarities with the striatal nuclei since those neurons are derived from a different source of progenitor cells. Dissimilarity of macro- and microstructure in the caudate and putamen may reflect differences in their subcortical location, particularly to the ventricles. Decreased WM integrity within the posterior limb of the internal capsule in SBM may result in increased interstitial space in the extracellular neuropil (Kriebel et al., 1993; Ou et al., 2011). The putamen is surrounded by the internal and external capsules, which may anchor the putamen and reduce displacement following hydrocephalus. However, compromised WM integrity of the internal capsule in individuals with SBM may allow for the putamen to expand.

While no group differences were observed for the thalamus or caudate volumes, these periventricular structures exhibited a similar pattern of increased MD and FA in the group with SBM. Given the proximity of these structures to the ventricles, increased MD and FA may suggest lower density and cellular degeneration following the mechanical effects of hydrocephalus. Periventricular WM disruption (stretching) is the most frequent consequence of hydrocephalus and results in atrophy and gliosis of periventricular WM, increased extracellular space, and neuronal degeneration (Del Bigio, 2010; Del Bigio et al., 2003; Kriebel et al., 1993). Neuropathological studies in hydrocephalic rats indicate that hydrocephalus severity is positively related to thalamic apoptosis following disrupted periventricular WM (Del Bigio, 2010; Mori et al., 2002). Potentially, our observations of increased MD and FA in the thalamus and caudate of children and adolescents with SBM may be explained by less densely packed cells resulting from induced cell death from hydrocephalus. Our finding of increased FA in the caudate in SBM corroborates preliminary findings from a subset of this cohort (Hasan et al., 2008b), which was interpreted as reflecting reduced dendritic branching.

4.1. Limitations

Functional outcomes across individuals with SBM vary greatly and may be complicated by hydrocephalus and associated shunting. As previously mentioned, hydrocephalus disrupts neural structure, regardless of etiology (Del Bigio, 2010; Scott et al., 1998; Yeates and Enrile, 2005). The majority of children and adolescents with SBM in the current sample had hydrocephalus and had histories of shunt surgery. The current findings of nonsignificant relations between macro- and microstructural values of GM and number of shunt revisions should be interpreted cautiously. Shunting procedures were not uniform across individuals with SBM in the current sample and can disrupt brain structure during insertion and, when applicable, revision. Both the location and number of revisions could have impacted brain structure. Future research could benefit from an examination of how, specifically, shunt insertion (and revision) alters neural structure in this population and whether shunt location influences these outcomes. Therefore, current results represent a complex, and potentially synergistic, interplay between neural tube defect (i.e., SBM), hydrocephalus (resulting from the characteristic Chiari II malformation), and shunting history.

The current study examined a fairly broad age range, although statistical attempts to account for age were made. Although age was not strongly associated with regional subcortical GM volumes, it was significantly associated with the DTI metric measurements in the majority of analyses. However, for most models, group accounted for a greater amount of variance than age. Additionally, the relations observed between age and GM microstructure (negative for MD and positive for FA) support previous literature (Lebel et al., 2008; Lenroot et al., 2007; Ostby et al., 2009). Methodological weaknesses include the sample size of the comparison group and the use of a less advanced neuroimaging protocol relative to contemporary standards. A larger comparison group of TD individuals would be desirable especially given the broad age-range assessed. Future research may also benefit from a more advanced imaging protocol, including the utilization of greater angular resolution by increasing the number of diffusion directions for the DTI acquisition. However, we feel that the current data acquisition and processing were sufficient to address the current analytic questions and were state of the art at the time of data collection. Lastly, while we did not assess for puberty, subsequent developmental changes could have

influenced findings, as subcortical GM development peaks after puberty (Lenroot et al., 2007). Future research would benefit from an investigation into the timing and hormonal effects of puberty on brain maturation in patients with SBM, particularly given reports of precocious puberty in this population (Meyer and Landau, 1984; Oakeshott and Hunt, 2003).

4.2. Implications and future directions

The current study examined the structural properties of deep GM in order to elucidate potential neural correlates underlying disrupted neurobehavioral outcomes. These findings are especially interesting given that these areas were largely read as normal in radiological review. Disruptions in higher-order cognition and motor functioning following SBM may be accounted for by aberrant development of subcortical GM. For instance, frontostriatal circuitry, which comprises the prefrontal, basal ganglia, and thalamic regions, is involved in multiple aspects of motor learning and control, including motor initiation, inhibition, and planning (Alexander et al., 1986). Additionally, the thalamus and certain basal ganglia nuclei, particularly the caudate and putamen, are shown to facilitate working memory and attentional control, which are impaired in individuals with SBM (Baier et al., 2010; Brown et al., 2008; Burmeister et al., 2005; Cohen and Frank, 2009; Rose and Holmbeck, 2007; Vachha and Adams, 2005). Furthermore, limbic system dysfunction, especially hippocampal, in SBM supports diminished memory abilities in this population (Dennis et al., 2007; Dennis et al., 2010; Hampton et al., 2011; Vachha and Adams, 2005; Vachha et al., 2006).

Overall, the present results support our concept of regionally specific brain areas being differentially impacted by this early gestational insult. However, the specific functional impairments associated with such structural abnormalities have yet to be identified. Examining neurobehavioral correlates of specific subcortical structures and the underlying behavioral differences observed in SBM would promote our understanding of these relations. Furthermore, while informative, macrostructural anomalies may only represent CNS damage associated with SBM, and do not explain complex interactions between regional microstructure in relation to global brain circuitry. Future research would significantly benefit from longitudinal investigations of subcortical GM development in children with SBM. Such investigations may illuminate mechanisms of plasticity and provide a foundation for effective intervention in this population.

Conflicts of interest

None to report.

Acknowledgments

This work was supported by the Eunice Kennedy Shriver National Institute of Child Health and Human Development Grant (P01 HD35946-06, “Spina Bifida: Cognitive and Neurobiological Variability”). The content is solely the responsibility of the authors and does not represent the official views of the Eunice Kennedy Shriver National Institute of Child Health and Human Development or the National Institute of Health.

References

Abe, O., Yamasue, H., Aoki, S., Suga, M., Yamada, H., Kasai, K., Masutani, Y., Kato, N., Kato, N., Ohtomo, K., 2008. Aging in the CNS: comparison of gray/white matter volume and diffusion tensor data. Neurobiology of Aging 29, 102–116. http://dx.doi.org/10.1016/j.neurobiolaging.2006.09.00317023094.

Alexander, G.E., DeLong, M.R., Strick, P.L., 1986. Parallel organization of functionally segregated circuits linking basal ganglia and cortex. Annual Review of Neuroscience 9, 357–381. http://dx.doi.org/10.1146/annurev.ne.09.030186.0020413085570.

Arnold, S.E., Trojanowski, J.Q., 1996. Human fetal hippocampal development: II. The neuronal cytoskeleton. Journal of Comparative Neurology 367, 293–307. http://dx.doi.org/10.1002/(SICI)1096-9861(19960401)367:2<293::AID-CNE10>3.0.CO;2-S8708011.

Au, K.S., Ashley-Koch, A., Northrup, H., 2010. Epidemiologic and genetic aspects of spina bifida and other neural tube defects. Developmental Disabilities Research Reviews 16, 6–15. http://dx.doi.org/10.1002/ddrr.9320419766.

Baier, B., Karnath, H.O., Dieterich, M., Birklein, F., Heinze, C., Muller, N.G., 2010. Keeping memory clear and stable—the contribution of human basal ganglia and prefrontal cortex to working memory. Journal of Neuroscience: the Official Journal of the Society for Neuroscience 30, 9788–9792. http://dx.doi.org/10.1523/JNEUROSCI.1513-10.201020660261.

Brown, T.M., Ris, M.D., Beebe, D., Ammerman, R.T., Oppenheimer, S.G., Yeates, K.O., Enrile, B.G., 2008. Factors of biological risk and reserve associated with executive behaviors in children and adolescents with spina bifida myelomeningocele. Child Neuropsychology: A Journal on Normal and Abnormal Development in Childhood and Adolescence 14, 118–134. http://dx.doi.org/10.1080/09297040601147605183060076.

Burmeister, R., Hannay, H.J., Copeland, K., Fletcher, J.M., Boudousquie, A., Dennis, M., 2005. Attention problems and executive functions in children with spina bifida and hydrocephalus. Child Neuropsychology: A Journal on Normal and Abnormal Development in Childhood and Adolescence 11, 265–283. http://dx.doi.org/10.1080/09297049091132416036451.

Cohen, M.X., Frank, M.J., 2009. Neurocomputational models of basal ganglia function in learning, memory and choice. Behavioural Brain Research 199, 141–156. http://dx.doi.org/10.1016/j.bbr.2008.09.02918950662.

Del, Bigio M.R., 2010. Neuropathology and structural changes in hydrocephalus. Developmental Disabilities Research Reviews 16, 16–22. http://dx.doi.org/10.1002/ddrr.9420419767.

Del, Bigio M.R., Wilson, M.J., Enno, T., 2003. Chronic hydrocephalus in rats and humans: white matter loss and behavior changes. Annals of Neurology 53, 337–346. http://dx.doi.org/10.1002/ana.1045312601701.

Del, Bigio M.R., Zhang, Y.W., 1998. Cell death, axonal damage, and cell birth in the immature rat brain following induction of hydrocephalus. Experimental Neurology 154, 157–169. http://dx.doi.org/10.1006/exnr.1998.69229875277.

Dennis, M., Barnes, M.A., 2010. The cognitive phenotype of spina bifida meningomyelocele. Developmental Disabilities Research Reviews 16, 31–39. http://dx.doi.org/10.1002/ddrr.8920419769.

Dennis, M., Edelstein, K., Hetherington, R., Copeland, K., Frederick, J., Blaser, S.E., Kramer, L.A., Drake, J.M., Brandt, M., Fletcher, J.M., 2004. Neurobiology of perceptual and motor timing in children with spina bifida in relation to cerebellar volume. Brain: A Journal of Neurology 127, 1292–1301. http://dx.doi.org/10.1093/brain/awh15415069019.

Dennis, M., Francis, D.J., Cirino, P.T., Schachar, R., Barnes, M.A., Fletcher, J.M., 2009. Why IQ is not a covariate in cognitive studies of neurodevelopmental disorders. Journal of the International Neuropsychological Society: JINS 15, 331–343. http://dx.doi.org/10.1017/S1355617709090481194029219.

Dennis, M., Jewell, D., Drake, J., Misakyan, T., Spiegler, B., Hetherington, R., Gentili, F., Barnes, M., 2007. Prospective, declarative, and nondeclarative memory in young adults with spina bifida. Journal of the International Neuropsychological Society: JINS 13, 312–32317286888.

Dennis, M., Nelson, R., Jewell, D., Fletcher, J.M., 2010. Prospective memory in adults with spina bifida. Child's Nervous System: ChNS: Official Journal of the International Society for Pediatric Neurosurgery 26, 1749–1755. http://dx.doi.org/10.1007/s00381-010-1140-z20393850.

Detrait, E.R., George, T.M., Etchevers, H.C., Gilbert, J.R., Vekemans, M., Speer, M.C., 2005. Human neural tube defects: developmental biology, epidemiology, and genetics. Neurotoxicology and Teratology 27, 515–524. http://dx.doi.org/10.1016/j.ntt.2004.12.00715939212.

Filipek, P.A., Kennedy, D.N., Caviness, V.S., Rossnick, S.L., Spraggins, T.A., Starewicz, P.M., 1989. Magnetic resonance imaging-based brain morphometry: development and application to normal subjects. Annals of Neurology 25, 61–67. http://dx.doi.org/10.1002/ana.4102501102643919.

Fischl, B., 2012. FreeSurfer. Neuroimage 62, 774–781. http://dx.doi.org/10.1016/j.neuroimage.2012.01.02122248573.

Fischl, B., Salat, D.H., Busa, E., Albert, M., Dieterich, M., Haselgrove, C., van, der Kouwe A., Killiany, R., Kennedy, D., Klaveness, S., Montillo, A., Makris, N., Rosen, B., Dale, A.M., 2002. Whole brain segmentation: automated labeling of neuroanatomical structures in the human brain. Neuron 33, 341–355. http://dx.doi.org/10.1016/S0896-6273(02)00569-X11832223.

Fischl, B., Salat, D.H., van, der Kouwe A.J., Makris, N., Segonne, F., Quinn, B.T., Dale, A.M., 2004a. Sequence-independent segmentation of magnetic resonance images. Neuroimage 23 (Suppl. 1), S69–S84. http://dx.doi.org/10.1016/j.neuroimage.2004.07.01615501102.

Fischl, B., van, der Kouwe A., Destrieux, C., Halgren, E., Segonne, F., Salat, D.H., Busa, E., Seidman, L.J., Goldstein, J., Kennedy, D., Caviness, V., Makris, N., Rosen, B., Dale, A.M., 2004b. Automatically parcellating the human cerebral cortex. Cerebral Cortex (New York, N.Y.: 1991) 14, 11–22. http://dx.doi.org/10.1093/cercor/bhg08714654453.

Fletcher, J.M., Copeland, K., Frederick, J.A., Blaser, S.E., Kramer, L.A., Northrup, H., Hannay, H.J., Brandt, M.E., Francis, D.J., Villarreal, G., Drake, J.M., Laurent, J.P., Townsend, I., Inwood, S., Boudousquie, A., Dennis, M., 2005. Spinal lesion level in spina bifida: a source of neural and cognitive heterogeneity. Journal of Neurosurgery 102, 268–27915881750.

Giedd, J.N., Blumenthal, J., Jeffries, N.O., Castellanos, F.X., Liu, H., Zijdenbos, A., Paus, T., Evans, A.C., Rapoport, J.L., 1999a. Brain development during childhood and adolescence: a longitudinal MRI study. Nature Neuroscience 2, 861–863. http://dx.doi.org/10.1038/13158.

Giedd, J.N., Blumenthal, J., Jeffries, N.O., Rajapakse, J.C., Vaituzis, A.C., Liu, H., Berry, Y.C., Tobin, M., Nelson, J., Castellanos, F.X., 1999b. Development of the human corpus callosum during childhood and adolescence: a longitudinal MRI study. Progress in Neuro-Psychopharmacology & Biological Psychiatry 23, 571–588. http://dx.doi.org/10.1016/S0278-5846(99)00017-210390717.

Good, C.D., Johnsrude, I.S., Ashburner, J., Henson, R.N., Friston, K.J., Frackowiak, R.S., 2001. A voxel-based morphometric study of ageing in 465 normal adult human brains. NeuroImage 14, 21–36. http://dx.doi.org/10.1006/nimg.2001.078611525331.

Hampton, L.E., Fletcher, J.M., Cirino, P.T., Blaser, S., Kramer, L.A., Drake, J., Dennis, M., 2011. Hydrocephalus status in spina bifida: an evaluation of variations in neuropsychological outcomes. Journal of Neurosurgery. Pediatrics 8, 289–298. http://dx.doi.org/10.3171/2011.6.PEDS1058421882921.

Hannay, H.J., Dennis, M., Kramer, L., Blaser, S., Fletcher, J.M., 2009. Partial agenesis of the corpus callosum in spina bifida meningomyelocele and potential compensatory mechanisms. Journal of Clinical and Experimental Neuropsychology 31, 180–194. http://dx.doi.org/10.1080/13803390802020995419052950.

Hannay, H.J., Walker, A., Dennis, M., Kramer, L., Blaser, S., Fletcher, J.M., 2008. Auditory interhemispheric transfer in relation to patterns of partial agenesis and hypoplasia of the corpus callosum in spina bifida meningomyelocele. Journal of the International Neuropsychological Society: JINS 14, 771–78118764972.

Hasan, K.M., Eluvathingal, T.J., Kramer, L.A., Ewing-Cobbs, L., Dennis, M., Fletcher, J.M., 2008a. White matter microstructural abnormalities in children with spina bifida myelomeningocele and hydrocephalus: a diffusion tensor tractography study of the association pathways. Journal of Magnetic Resonance Imaging: JMRI 27, 700–709. http://dx.doi.org/10.1002/jmri.2129718302204.

Hasan, K.M., Sankar, A., Halphen, C., Kramer, L.A., Ewing-Cobbs, L., Dennis, M., Fletcher, J.M., 2008b. Quantitative diffusion tensor imaging and intellectual outcomes in spina bifida: laboratory investigation. Journal of Neurosurgery. Pediatrics 2, 75–82. http://dx.doi.org/10.3171/PED/2008/2/7/07518590401.

Herweh, C., Akbar, M., Wengenroth, M., Blatow, M., Mair-Walther, J., Rehbein, N., Nennig, E., Schenk, J.P., Heiland, S., Stippich, C., 2009. DTI of commissural fibers in patients with Chiari II-malformation. Neuroimage 44, 306–311. http://dx.doi.org/10.1016/j.neuroimage.2008.09.00618849000.

Hollingshead, A.B., Four Factor Index of Social Status. Unpublished Working Paper (1975).

Jenkinson, M., Bannister, P., Brady, M., Smith, S., 2002. Improved optimization for the robust and accurate linear registration and motion correction of brain images. Neuroimage 17, 825–841. http://dx.doi.org/10.1006/nimg.2002.113212377157.

Juranek, J., Fletcher, J.M., Hasan, K.M., Breier, J.I., Cirino, P.T., Pazo-Alvarez, P., Diaz, J.D., Ewing-Cobbs, L., Dennis, M., Papanicolaou, A.C., 2008. Neocortical reorganization in spina bifida. NeuroImage 40, 1516–1522. http://dx.doi.org/10.1016/j.neuroimage.2008.01.04318337124.

Juranek, J., Johnson, C.P., Prasad, M.R., Kramer, L.A., Saunders, A., Filipek, P.A., Swank, P.R., Cox Jr., C.S., Ewing-Cobbs, L., 2012. Mean diffusivity in the amygdala correlates with anxiety in pediatric TBI. Brain Imaging and Behavior 6, 36–48. http://dx.doi.org/10.1007/s11682-011-9140-521979818.

Juranek, J., Salman, M.S., 2010. Anomalous development of brain structure and function in spina bifida myelomeningocele. Developmental Disabilities Research Reviews 16, 23–30. http://dx.doi.org/10.1002/ddrr.8820419768.

Kriebel, R.M., McAllister 2nd, J.P., 2000. Pathology of the hippocampus in experimental feline infantile hydrocephalus. Neurological Research 22, 29–3610672578.

Kriebel, R.M., Shah, A.B., McAllister 2nd, J.P., 1993. The microstructure of cortical neuropil before and after decompression in experimental infantile hydrocephalus. Experimental Neurology 119, 89–98. http://dx.doi.org/10.1006/exnr.1993.10098432354.

Kumar, M., Gupta, R.K., Saksena, S., Behari, S., Malik, G.K., Kureel, S.N., Pandey, C.M., Rathore, R.K., 2010. A diffusion tensor imaging study of deep gray and white matter brain maturation differences between patients with spina bifida cystica and healthy controls. Journal of Clinical Neuroscience: Official Journal of the Neurosurgical Society of Australasia 17, 879–885. http://dx.doi.org/10.1016/j.jocn.2009.09.04120400314.

Kumar, M., Srivastava, A., Agarwal, S., Behari, S., Malik, G.K., Rathore, R.K., Gupta, R.K., 2011. Cognitive functions correlate with diffusion tensor imaging metrics in patients with spina bifida cystica. Child's Nervous System: ChNS: Official Journal of the International Society for Pediatric Neurosurgery 27, 723–728. http://dx.doi.org/10.1007/s00381-010-1329-121080174.

Kutner, M.H., Nachtsheim, C.J., Neter, J., Li, W., 2005. Applied Linear Statistical Modelsfifth edition. McGraw-Hill/Irwin, New York, NY.

Lebel, C., Walker, L., Leemans, A., Phillips, L., Beaulieu, C., 2008. Microstructural maturation of the human brain from childhood to adulthood. NeuroImage 40, 1044–1055. http://dx.doi.org/10.1016/j.neuroimage.2007.12.05318295509.

Lenroot, R.K., Gogtay, N., Greenstein, D.K., Wells, E.M., Wallace, G.L., Clasen, L.S., Blumenthal, J.D., Lerch, J., Zijdenbos, A.P., Evans, A.C., Thompson, P.M., Giedd, J.N., 2007. Sexual dimorphism of brain developmental trajectories during childhood and adolescence. Neuroimage 36, 1065–1073. http://dx.doi.org/10.1016/j.neuroimage.2007.03.05317513132.

Mataro, M., Poca, M.A., Matarin, M., Sahuquillo, J., Sebastian, N., Junque, C., 2006. Corpus callosum functioning in patients with normal pressure hydrocephalus before and after surgery. Journal of Neurology 253, 625–630. http://dx.doi.org/10.1007/s00415-005-0073-z16362531.

Marín, O., Rubenstein, J.L.R., 2003. Cell migration in the forebrain. Annual Review of Neuroscience 26 (1), 441–483. http://dx.doi.org/10.1146/annurev.neuro.26.041002.131058.

Meyer, S., Landau, H., 1984. Precocious puberty in myelomeningocele patients. Journal of Pediatric Orthopedics 4, 28–31. http://dx.doi.org/10.1097/01241398-198401000-000076141180.

Morgane, P.J., Mokler, D.J., Galler, J.R., 2002. Effects of prenatal protein malnutrition on the hippocampal formation. Neuroscience and Biobehavioral Reviews 26, 471–483. http://dx.doi.org/10.1016/S0149-7634(02)00012-X12204193.

Mori, K., Maeda, M., Asegawa, S., Iwata, J., 2002. Quantitative local cerebral blood flow change after cerebrospinal fluid removal in patients with normal pressure hydrocephalus measured by a double injection method with N-isopropyl-p-[(123)I] iodoamphetamine. Acta Neurochirurgica (Wien) 144, 255–262. http://dx.doi.org/10.1007/s007010200033.

Mukherjee, P., Miller, J.H., Shimony, J.S., Philip, J.V., Nehra, D., Snyder, A.Z., Conturo, T.E., Neil, J.J., McKinstry, R.C., 2002. Diffusion-tensor MR imaging of gray and white matter development during normal human brain maturation. AJNR. American Journal of Neuroradiology 23, 1445–145612372731.

Müller, F., O'Rahilly, R., 2006. The amygdaloid complex and the medial and lateral ventricular eminences in staged human embryos. Journal of Anatomy 208 (5), 547–564. http://dx.doi.org/10.1111/j.1469-7580.2006.00553.x16637878.

Naidich, T.P., McLone, D.G., Hahn, Y.S., Hanaway, J., 1982. Atrial diverticula in severe hydrocephalus. AJNR. American Journal of Neuroradiology 3, 257–2666805275.

Oakeshott, P., Hunt, G.M., 2003. Long-term outcome in open spina bifida. British Journal of General Practice: the Journal of the Royal College of General Practitioners 53, 632–63614601340.

Ostby, Y., Tamnes, C.K., Fjell, A.M., Westlye, L.T., Due-Tonnessen, P., Walhovd, K.B., 2009. Heterogeneity in subcortical brain development: a structural magnetic resonance imaging study of brain maturation from 8 to 30 years. Journal of Neuroscience: the Official Journal of the Society for Neuroscience 29, 11772–11782. http://dx.doi.org/10.1523/JNEUROSCI.1242-09.200919776264.

Ou, X., Glasier, C.M., Snow, J.H., 2011. Diffusion tensor imaging evaluation of white matter in adolescents with myelomeningocele and Chiari II malformation. Pediatric Radiology 41, 1407–1415. http://dx.doi.org/10.1007/s00247-011-2180-621725712.

Rose, B.M., Holmbeck, G.N., 2007. Attention and executive functions in adolescents with spina bifida. Journal of Pediatric Psychology 32, 983–994. http://dx.doi.org/10.1093/jpepsy/jsm04217556398.

Ross, G., Lipper, E.G., Auld, P.A., 1987. Hand preference of four-year-old children: its relationship to premature birth and neurodevelopmental outcome. Developmental Medicine and Child Neurology 29, 615–6222444483.

Scott, M.A., Fletcher, J.M., Brookshire, B.L., Davidson, K.C., Landry, S.H., Bohan, T.C., Kramer, L.A., Brandt, M.E., Francis, D.J., 1998. Memory functions in children with early hydrocephalus. Neuropsychology 12, 578–589. http://dx.doi.org/10.1037/0894-4105.12.4.5789805328.

Smith, S.M., Jenkinson, M., Woolrich, M.W., Beckmann, C.F., Behrens, T.E., Johansen-Berg, H., Bannister, P.R., De, Luca M., Drobnjak, I., Flitney, D.E., Niazy, R.K., Saunders, J., Vickers, J., Zhang, Y., De, Stefano N., Brady, J.M., Matthews, P.M., 2004. Advances in functional and structural MR image analysis and implementation as FSL. Neuroimage 23 (Suppl. 1), S208–S219. http://dx.doi.org/10.1016/j.neuroimage.2004.07.05115501092.

Thorndike, R., Hagen, E., Sattler, J., 1986. The Stanford–Binet Intelligence ScaleRiverside, Itasca, IL.

Treble, A., Juranek, J., Stuebing, K.K., Dennis, M., Fletcher, J.M., 2013. Functional significance of atypical cortical organization in spina bifida myelomeningocele: relations of cortical thickness and gyrification with IQ and fine motor dexterity. Cerebral Cortex (New York, N.Y.: 1991) 23, 2357–2369. http://dx.doi.org/10.1093/cercor/bhs22622875857.

Vachha, B., Adams, R.C., 2005. Memory and selective learning in children with spina bifida-myelomeningocele and shunted hydrocephalus: a preliminary study. Cerebrospinal Fluid Research 2, 10. http://dx.doi.org/10.1186/1743-8454-2-1016293188.

Vachha, B., Adams, R.C., Rollins, N.K., 2006. Limbic tract anomalies in pediatric myelomeningocele and Chiari II malformation: anatomic correlations with memory and learning—initial investigation. Radiology 240, 194–202. http://dx.doi.org/10.1148/radiol.240105067416793979.

Williams, V.J., Juranek, J., Stuebing, K., Cirino, P.T., Dennis, M., Fletcher, J.M., 2013. Examination of frontal and parietal tectocortical attention pathways in spina bifida meningomyelocele using probabilistic diffusion tractography. Brain Connectivity 3, 512–522. http://dx.doi.org/10.1089/brain.2013.017123937233.

Yeates, K.O., Enrile, B.G., 2005. Implicit and explicit memory in children with congenital and acquired brain disorder. Neuropsychology 19, 618–628. http://dx.doi.org/10.1037/0894-4105.19.5.61816187880.